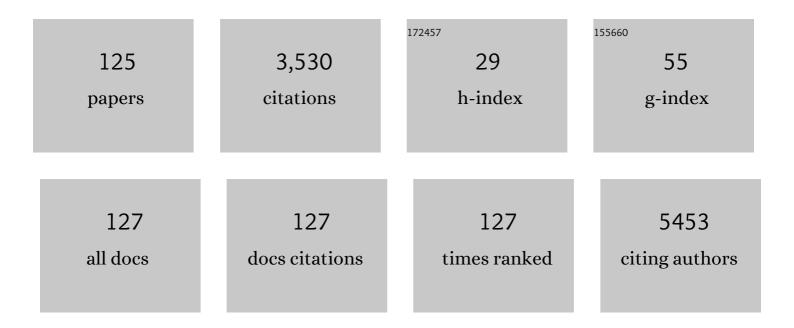


## List of Publications by Year in descending order

Source: https://exaly.com/author-pdf/619378/publications.pdf Version: 2024-02-01



#	Article	IF	CITATIONS
1	A concise guide to scheduling with learning and deteriorating effects. International Journal of Production Research, 2023, 61, 2010-2031.	7.5	8
2	Preparation and electrocatalytic performance of N-doped hierarchical porous carbon loaded with Fe/Fe5C2 nanoparticles. Journal of Alloys and Compounds, 2022, 903, 163874.	5.5	7
3	Synthesis and excellent performance of porous <scp> Ni <sub>2</sub> P </scp> @C/ <scp>CNTs</scp> nanocomposite derived from <scp>Niâ€MOFs</scp> as an anode for lithiumâ€ion batteries. International Journal of Energy Research, 2022, 46, 10875-10884.	4.5	3
4	10 kW Fiber Amplifier Seeded by Random Fiber Laser With Suppression of Spectral Broadening and SRS. IEEE Photonics Technology Letters, 2022, 34, 721-724.	2.5	14
5	A dual-targeting Fe3O4@C/ZnO-DOX-FA nanoplatform with pH-responsive drug release and synergetic chemo-photothermal antitumor in vitro and in vivo. Materials Science and Engineering C, 2021, 118, 111455.	7.3	17
6	Deeply reconstructed hierarchical and defective NiOOH/FeOOH nanoboxes with accelerated kinetics for the oxygen evolution reaction. Journal of Materials Chemistry A, 2021, 9, 15586-15594.	10.3	162
7	Application of mouse model for evaluation of recombinant LpxC and GmhA as novel antigenic vaccine candidates of <i>Glaesserella parasuis</i> serotype 13. Journal of Veterinary Medical Science, 2021, 83, 1500-1508.	0.9	3
8	Self-assembled Au <sub>4</sub> Cu <sub>4</sub> /Au <sub>25</sub> NCs@liposome tumor nanotheranostics with PT/fluorescence imaging-guided synergetic PTT/PDT. Journal of Materials Chemistry B, 2021, 9, 6396-6405.	5.8	21
9	In-situ preparation of Ferrero® chocolate-like Cu2O@Ag microsphere as SERS substrate for detection of thiram. Journal of Materials Research and Technology, 2021, 11, 857-865.	5.8	26
10	Synthesis and superior SERS performance of porous octahedron Cu2O with oxygen vacancy derived from MOFs. Journal of Materials Science, 2021, 56, 9702-9711.	3.7	12
11	Porous Co/NPC@TiO2/TiN composite: Facile preparation and excellent catalytic activity for the oxygen reduction reaction. Journal of Alloys and Compounds, 2021, 883, 160838.	5.5	4
12	An effective NIR laser/tumor-microenvironment co-responsive cancer theranostic nanoplatform with multi-modal imaging and therapies. Nanoscale, 2021, 13, 10816-10828.	5.6	18
13	SnO2/Bi2O3/NF heterojunction with ordered macro/meso-pore structure as an advanced binder-free anode for lithium ion batteries. Journal of Electroanalytical Chemistry, 2021, 907, 115894.	3.8	7
14	Octagonal Flowerâ€like CuO/C/NF Nanocomposite as a Self‣upporting Anode for Highâ€Performance Lithiumâ€lon Batteries. ChemElectroChem, 2020, 7, 4038-4046.	3.4	6
15	Structurally accurate lipophilic Pt1Ag28 nanoclusters based cancer theranostic micelles for dual-targeting/aggregation enhanced fluorescence imaging and photothermal/photodynamic therapies. Colloids and Surfaces B: Biointerfaces, 2020, 196, 111346.	5.0	10
16	In-situ preparation and excellent performance of Co9S8/C/NF with binder-free as anodes for lithium-ion batteries. Journal of Materials Research and Technology, 2020, 9, 10679-10685.	5.8	5
17	A structurally precise Ag <sub>x</sub> Au <sub>25â^'x</sub> nanocluster based cancer theranostic platform with tri-targeting/ <i>in situ</i> O <sub>2</sub> -generation/aggregation enhanced fluorescence imaging/photothermal–photodynamic therapies. Chemical Communications, 2020, 56, 9842-9845.	4.1	11
18	A novel high doxorubicin-loaded Fe3O4@void@ZnO nanocomposite: pH-controlled drug release and targeted antitumor activity. Journal of Materials Science, 2020, 55, 16718-16729.	3.7	3

#	Article	IF	CITATIONS
19	Interconnected porous nitrogen-doped carbon framework: Recoverable template fabrication and excellent electrocatalytic performance for oxygen reduction reaction. Journal of the Taiwan Institute of Chemical Engineers, 2020, 113, 178-186.	5.3	4
20	Yolk-shelled FeP/Ni2P/C@C nanospheres with void: Controllable synthesis and excellent performance as the anode for lithium-ion batteries. Colloids and Surfaces A: Physicochemical and Engineering Aspects, 2020, 602, 125103.	4.7	7
21	Porous CoP@N/P co-doped carbon/CNTs nanocubes: In-situ autocatalytic synthesis and excellent performance as the anode for lithium-ion batteries. Applied Surface Science, 2020, 513, 145777.	6.1	44
22	4-in-1 phototheranostics: PDA@CoPA-LA nanocomposite for photothermal imaging/photothermal/in-situ O2 generation/photodynamic combination therapy. Chemical Engineering Journal, 2020, 387, 124113.	12.7	27
23	An Efficient Non-Invasive Method to Fabricate In-Fiber Microcavities Using a Continuous-Wave Laser. IEEE Photonics Technology Letters, 2020, 32, 573-576.	2.5	1
24	Ni3S2@Graphene oxide nanosheet arrays grown on NF as binder-free anodes for lithium ion batteries. Journal of Alloys and Compounds, 2019, 810, 151861.	5.5	15
25	Exploring the initiation of fiber fuse. Scientific Reports, 2019, 9, 11655.	3.3	10
26	Inâ€Situ Synthesis and Electrocatalytic Performance of Fe/Fe <sub>2.5</sub> C/Fe <sub>3</sub> N/Nitrogenâ€Đoped Carbon Nanotubes for the Oxygen Reduction Reaction. ChemElectroChem, 2019, 6, 3030-3038.	3.4	8
27	In-Situ Synthesis of Petal-Like MoO <sub>2</sub> @MoN/NF Heterojunction As Both an Advanced Binder-Free Anode and an Electrocatalyst for Lithium Ion Batteries and Water Splitting. ACS Sustainable Chemistry and Engineering, 2019, 7, 9153-9163.	6.7	36
28	A novel FeC2O4-TOP derived porous pillar-like $\hat{I}^3$ -Fe2O3/carbon nanocomposite with excellent performance as anode for lithium-ion batteries. Applied Surface Science, 2019, 479, 1212-1219.	6.1	15
29	Beam Transmission Properties in High Power Ytterbium-Doped Tandem-Pumping Fiber Amplifier. IEEE Photonics Journal, 2019, 11, 1-12.	2.0	6
30	Effective photodynamic therapy of polymer hydrogel on tumor cells prepared using methylene blue sensitized mesoporous titania nanocrystal. Materials Science and Engineering C, 2019, 99, 1392-1398.	7.3	17
31	B, N Coâ€Đoped Threeâ€Dimensional Carbon Aerogels with Excellent Electrochemical Performance for the Oxygen Reduction Reaction. Chemistry - A European Journal, 2019, 25, 2877-2883.	3.3	31
32	Developing cysteamine-modified SERS substrate for detection of acidic pigment with weak surface affinity. Spectrochimica Acta - Part A: Molecular and Biomolecular Spectroscopy, 2019, 212, 293-299.	3.9	15
33	A novel bi-functional SiO2@TiO2/CDs nanocomposite with yolk-shell structure as both efficient SERS substrate and photocatalyst. Applied Surface Science, 2019, 475, 135-142.	6.1	15
34	Rapid Synthesis and Good Performance of TiO <sub>2</sub> /Nitrogenâ€Doped Carbon Spheres as Anode Materials for Lithium Ion Batteries. Energy Technology, 2018, 6, 1660-1666.	3.8	5
35	Hollow porous CuO/C nanorods as a high-performance anode for lithium ion batteries. Journal of Alloys and Compounds, 2018, 750, 77-84.	5.5	25
36	Facile synthesis and electrochemical performance of nitrogen-doped porous hollow coaxial carbon fiber/Co3O4 composite. Ceramics International, 2018, 44, 5848-5854.	4.8	10

#	Article	IF	CITATIONS
37	In situ synthesis of nori-derived sponge-like N, P-codoped C/Co3O4 composite as advanced anode material for lithium-ion batteries. Journal of Alloys and Compounds, 2018, 740, 446-451.	5.5	12
38	Highly ordered ZnO/ZnFe <sub>2</sub> O <sub>4</sub> inverse opals with binder-free heterojunction interfaces for high-performance photoelectrochemical water splitting. Journal of Materials Chemistry A, 2018, 6, 1210-1218.	10.3	73
39	EGCG Reduces Obesity and White Adipose Tissue Gain Partly Through AMPK Activation in Mice. Frontiers in Pharmacology, 2018, 9, 1366.	3.5	113
40	Construction and synergistic anticancer efficacy of magnetic targeting cabbage-like Fe <sub>3</sub> O <sub>4</sub> @MoS <sub>2</sub> @ZnO drug carriers. Journal of Materials Chemistry B, 2018, 6, 3792-3799.	5.8	20
41	A novel 5-FU/rGO/Bce hybrid hydrogel shell on a tumor cell: one-step synthesis and synergistic chemo/photo-thermal/photodynamic effect. RSC Advances, 2017, 7, 2415-2425.	3.6	8
42	Reduced Graphene Oxide@Mesoporous Silica–Doxorubicin/Hydroxyapatite Inorganic Nanocomposites: Preparation and pH–Light Dualâ€īriggered Synergistic Chemoâ€Photothermal Therapy. European Journal of Inorganic Chemistry, 2017, 2017, 2236-2246.	2.0	16
43	Graphene oxide and creatine phosphate disodium dual template-directed synthesis of GO/hydroxyapatite and its application in drug delivery. Materials Science and Engineering C, 2017, 73, 709-715.	7.3	36
44	Novel porous starfish-like Co3O4@nitrogen-doped carbon as an advanced anode for lithium-ion batteries. Nano Research, 2017, 10, 3457-3467.	10.4	75
45	A novel composite hydrogel initiated by Spinacia oleracea L. extract on Hela cells for localized photodynamic therapy. Materials Science and Engineering C, 2017, 75, 1448-1455.	7.3	11
46	Photosensitive multifunctional poly(vinyl alcohol) micelles for enhanced antitumor effect. Materials Science and Engineering C, 2017, 76, 918-924.	7.3	6
47	RGO/AuNR/HA-5FU nanocomposite with multi-stage release behavior and efficient antitumor activity for synergistic therapy. Biomaterials Science, 2017, 5, 990-1000.	5.4	19
48	Litchi-like Fe <sub>3</sub> O <sub>4</sub> @Fe-MOF capped with HAp gatekeepers for pH-triggered drug release and anticancer effect. Journal of Materials Chemistry B, 2017, 5, 8600-8606.	5.8	58
49	Preparation and electromagnetic wave absorption of RGO/Cu nanocomposite. Russian Journal of Physical Chemistry A, 2017, 91, 1771-1774.	0.6	2
50	A GO@PLA@HA Composite Microcapsule: Its Preparation and Multistage and Controlled Drug Release. European Journal of Inorganic Chemistry, 2017, 2017, 3312-3321.	2.0	16
51	Spinach juice-derived porous Fe2O3/carbon nanorods as superior anodes for lithium-ion batteries. Materials Research Bulletin, 2017, 95, 321-327.	5.2	18
52	Facile synthesis and excellent electromagnetic wave absorption properties of flower-like porous RGO/PANI/Cu2O nanocomposites. Journal of Materials Science, 2017, 52, 13078-13090.	3.7	41
53	An effective strategy for the preparation of nitrogen-doped carbon from Imperata cylindrica panicle and its use as a metal-free catalyst for the oxygen reduction reaction. Energy, 2017, 141, 1324-1331.	8.8	7
54	A novel octaethylporphrin platinum sensitized TiO2 inverse opal: Construction and enhanced photoelectrochemical performance and photocatalytic activity. Molecular Catalysis, 2017, 443, 179-185.	2.0	0

#	Article	IF	CITATIONS
55	A pH-Sensitive Composite with Controlled Multistage Drug Release for Synergetic Photothermal Therapy and Chemotherapy. European Journal of Inorganic Chemistry, 2017, 2017, 5621-5628.	2.0	6
56	Synthesis of hollow magnetic and luminescent bifunctional composite nanoparticles. Colloid Journal, 2016, 78, 156-163.	1.3	6
57	3D and ternary rGO/MCNTs/Fe3O4 composite hydrogels: Synthesis, characterization and their electromagnetic wave absorption properties. Journal of Alloys and Compounds, 2016, 665, 381-387.	5.5	145
58	A novel porous aspirin-loaded (GO/CTS-HA) n nanocomposite films: Synthesis and multifunction for bone tissue engineering. Carbohydrate Polymers, 2016, 153, 124-132.	10.2	30
59	High-activity oxygen reduction catalyst based on low-cost bagasse, nitrogen and large specific surface area. Energy, 2016, 115, 397-403.	8.8	30
60	A Novel 2D Porous Print Fabric-like α-Fe2O3 Sheet with High Performance as the Anode Material for Lithium-ion Battery. Electrochimica Acta, 2016, 212, 912-920.	5.2	50
61	Novel template-free synthesis of hollow@porous TiO2 superior anode materials for lithium ion battery. Journal of Materials Science, 2016, 51, 3448-3453.	3.7	25
62	A novel reducing graphene/polyaniline/cuprous oxide composite hydrogel with unexpected photocatalytic activity for the degradation of Congo red. Applied Surface Science, 2016, 360, 594-600.	6.1	80
63	A facile strategy for the preparation of a porous flower-like Fe 3 O 4 /Cu 2 O/Ag nanocomposite with unexpected and recyclable photocatalytic activity under visible light irradiation. Materials Letters, 2016, 163, 106-110.	2.6	7
64	One-pot synthesis and photoluminescence properties of core/porous-shell olive-like BaWO4 microstructure by a template-assisted hydrothermal method. Russian Journal of Physical Chemistry A, 2016, 90, 498-503.	0.6	0
65	Nitrogen-doped nanoporous carbon derived from waste pomelo peel as a metal-free electrocatalyst for the oxygen reduction reaction. Nanoscale, 2016, 8, 8704-8711.	5.6	78
66	Facile synthesis and electrochemical properties of MoO 2 /reduced graphene oxide hybrid for efficient anode of lithium-ion battery. Ceramics International, 2016, 42, 3618-3624.	4.8	22
67	The Effect of Regeneration Techniques on Periapical Surgery With Different Protocols for Different Lesion Types: A Meta-Analysis. Journal of Oral and Maxillofacial Surgery, 2016, 74, 239-246.	1.2	16
68	A novel synthesis of ZnO/N-doped reduced graphene oxide composite as superior anode material for lithium-ion batteries. Scripta Materialia, 2016, 112, 67-70.	5.2	16
69	Layerâ€byâ€layer assembly of {chitosan/Pd} <sub>n</sub> multilayer film based on <i>inâ€situ</i> photochemical reduction with excellent electrocatalytic properties. Surface and Interface Analysis, 2015, 47, 1114-1119.	1.8	2
70	Reduced Graphene Oxide/Amaranth Extract/AuNPs Composite Hydrogel on Tumor Cells as Integrated Platform for Localized and Multiple Synergistic Therapy. ACS Applied Materials & Interfaces, 2015, 7, 11246-11256.	8.0	52
71	Morphology control and mechanisms of CaCO3 crystallization on gas-liquid interfaces of CO2/NH3 bubbles in aqueons-glycine solutions. Russian Journal of Physical Chemistry A, 2015, 89, 1091-1095.	0.6	2
72	Nacre-like calcium carbonate controlled by ionic liquid/graphene oxide composite template. Materials Science and Engineering C. 2015, 51, 274-278.	7.3	13

#	Article	IF	CITATIONS
73	Self-healable hydrogel on tumor cell as drug delivery system for localized and effective therapy. Carbohydrate Polymers, 2015, 122, 336-342.	10.2	78
74	Hierarchical flower-like Bi <sub>2</sub> WO <sub>6</sub> hollow microspheres: facile synthesis and excellent catalytic performance. RSC Advances, 2015, 5, 23080-23085.	3.6	14
75	Graphene oxide used as a surfactant to induce the flowerâ€like ZnO microstructures: growth mechanism and enhanced photocatalytic properties. Crystal Research and Technology, 2014, 49, 982-989.	1.3	16
76	Bioinspired synthesis of novel teethâ€ŀike hierarchical architecture polyaniline/lead tungstate nanocomposites with photoluminescence property. Polymer Composites, 2014, 35, 516-522.	4.6	3
77	Development of 2-Chlorophenol Sensor Based on a Fiber Optic Oxygen Transducer via Oxidation Reaction Catalyzed by Tetranitro Iron (II) Phthalocyanine. IEEE Sensors Journal, 2014, 14, 3693-3700.	4.7	3
78	Green synthesis and surface properties of Fe3O4@SA core–shell nanocomposites. Applied Surface Science, 2014, 301, 244-249.	6.1	17
79	Room temperature fabrication of an RGO–Fe3O4 composite hydrogel and its excellent wave absorption properties. RSC Advances, 2014, 4, 14441.	3.6	42
80	Preparation and Multiple Antitumor Properties of AuNRs/Spinach Extract/PEGDA Composite Hydrogel. ACS Applied Materials & Interfaces, 2014, 6, 15000-15006.	8.0	20
81	Multifunctional SERS substrates of Fe <sub>3</sub> O <sub>4</sub> @Ag <sub>2</sub> Se/Ag: construction, properties and application. Analytical Methods, 2014, 6, 7083.	2.7	6
82	Crystal growth of calcium carbonate on the cellulose acetate/pyrrolidon blend films in the presence of L-aspartic acid. Russian Journal of Physical Chemistry A, 2014, 88, 515-520.	0.6	0
83	One-pot synthesis of novel Fe3O4/Cu2O/PANI nanocomposites as absorbents in water treatment. Journal of Materials Chemistry A, 2014, 2, 7953.	10.3	51
84	Preparing and physicochemical properties of microcrystalline polyacrylic acid gels. Russian Journal of Physical Chemistry A, 2013, 87, 2100-2104.	0.6	3
85	Controlled fabrication of transparent and superhydrophobic coating on a glass matrix via a Green method. Applied Physics A: Materials Science and Processing, 2013, 110, 397-401.	2.3	10
86	A New Postprocessing Strategy for Secondary Pollution: Synthesis of CdS Crystals. Separation Science and Technology, 2012, 47, 684-687.	2.5	0
87	Complex calcium carbonate aggregates: controlled crystallization and assemblyvia an additive-modified positive-microemulsion-route. CrystEngComm, 2012, 14, 1277-1282.	2.6	9
88	Functionalization of cotton fabrics with rutile TiO2 nanoparticles: Applications for superhydrophobic, UV-shielding and self-cleaning properties. Russian Journal of Physical Chemistry A, 2012, 86, 413-417.	0.6	31
89	A simple method for preparation of transparent hydrophobic silica-based coatings on different substrates. Applied Physics A: Materials Science and Processing, 2012, 106, 229-235.	2.3	31
90	Novel structure CuI/PANI nanocomposites with bifunctions: superhydrophobicity and photocatalytic activity. Journal of Materials Chemistry, 2011, 21, 9641.	6.7	85

#	Article	IF	CITATIONS
91	Controlled synthesis, growth mechanism and optical properties of FeWO4 hierarchical microstructures. CrystEngComm, 2011, 13, 5744.	2.6	46
92	Fabrication of Superhydrophobic Cotton Fabrics with UV Protection Based on CeO <sub>2</sub> Particles. Industrial & Engineering Chemistry Research, 2011, 50, 4441-4445.	3.7	87
93	Miscibility of ethyl cellulose/copolyamide6/66/1010 blends by viscometry and refractive index method. Russian Journal of Physical Chemistry A, 2011, 85, 617-620.	0.6	1
94	Morphology control of anglesite microcrystals with polyhedron: Synthesis, growth mechanism, and optical properties. Russian Journal of Physical Chemistry A, 2011, 85, 1454-1464.	0.6	3
95	Sorption mechanisms of cadmium onto nano-hydroxyapatite: Comparative uptake studies and correlative solubility analysis. Russian Journal of Physical Chemistry A, 2011, 85, 1635-1640.	0.6	3
96	Fabrication and characterizations of mesoporous TiO2 and SiO2/TiO2 composite with high photocatalytic activity using a new Gemini surfactant. Russian Journal of Physical Chemistry A, 2011, 85, 2033-2037.	0.6	0
97	Biomimetic growth of CaCO3 pancakes on the leaves of Epipremnum aureum. Russian Journal of Physical Chemistry A, 2011, 85, 2187-2191.	0.6	1
98	Biomimetic synthesis of the arachidic acid/Ag x Cd y S nanocomposite films. Colloid Journal, 2011, 73, 784-787.	1.3	0
99	Facile fabrication and optical property of β-Bi2O3 with novel porous nanoring and nanoplate superstructures. Journal of Nanoparticle Research, 2011, 13, 4575-4582.	1.9	12
100	Synthesis and characterization of mesoporous silica using new gemini surfactants as templates in neutral pH conditions. International Journal of Materials Research, 2011, 102, 1493-1498.	0.3	0
101	Soft template inducing synthesis of CaC2O4 nanotubes. Russian Journal of Inorganic Chemistry, 2010, 55, 1953-1956.	1.3	1
102	Synthesis and characterization of PbS nanotubes in bicontinuous microemulsion system. Colloid Journal, 2010, 72, 274-278.	1.3	2
103	A novel method to realize the transition from silver nanowires to nanoplates based on the degradation of DNA. Journal of Nanoparticle Research, 2010, 12, 2679-2687.	1.9	2
104	Seed-Mediated Synthesis of Unusual Struvite Hierarchical Superstructures Using Bacterium. Crystal Growth and Design, 2010, 10, 2073-2082.	3.0	37
105	Synthesis of flakeâ€like crystals by a hydrothermal process. Crystal Research and Technology, 2009, 44, 409-413.	1.3	3
106	Controlled deposition and transformation of amorphous calcium carbonate thin films. Crystal Research and Technology, 2009, 44, 818-822.	1.3	4
107	Morphogenesis of Cul Nanocrystals by a TSAâ€Assisted Photochemical Route: Synthesis, Optical Properties, and Growth Mechanism. European Journal of Inorganic Chemistry, 2009, 2009, 1376-1384.	2.0	11
108	Effect of ethylene glycol on micellization and micellar-catalyzed alkaline hydrolysis reaction of a cationic surfactant at 293–313 K. Russian Journal of Physical Chemistry A, 2009, 83, 2238-2242.	0.6	0

#	Article	IF	CITATIONS
109	Synthesis and characterization of PbS nanorods in W/O microemulsion system. Russian Journal of Physical Chemistry A, 2009, 83, 2297-2301.	0.6	3
110	Tunable surface plasmon resonance of Au@Ag2S core–shell nanostructures containing voids. Journal of Materials Chemistry, 2009, 19, 8871.	6.7	37
111	Bacteria-Mediated Synthesis of Metal Carbonate Minerals with Unusual Morphologies and Structures. Crystal Growth and Design, 2009, 9, 743-754.	3.0	76
112	Synthesis of rhombohedral strontium carbonate aggregates at the water/hexamethylene interface with cetyltrimethylammonium bromide. Crystal Research and Technology, 2008, 43, 797-800.	1.3	10
113	Green synthesis of silver nanoparticles using Capsicum annuum L. extract. Green Chemistry, 2007, 9, 852.	9.0	844
114	Growth of calcium oxalate crystals induced by complex films containing biomolecules. Crystal Research and Technology, 2007, 42, 667-672.	1.3	7
115	Influence ofBacillus subtilis on the growth of calcium oxalate. Crystal Research and Technology, 2007, 42, 881-885.	1.3	16
116	Nanosized barium carbonate particles stabilized by cetyltrimethylammonium bromide at the water/hexamethylene interface. Crystal Research and Technology, 2007, 42, 886-889.	1.3	38
117	Synthesis of Controllable-Size Core–Shell Se@Ag and Se@Au Nanoparticles in UV-Irradiated TSA Solution. European Journal of Inorganic Chemistry, 2007, 2007, 1128-1134.	2.0	13
118	Oriented Attachment Growth of Three-Dimensionally Packed Trigonal Selenium Microspheres into Large-Area Wire Networks. European Journal of Inorganic Chemistry, 2007, 2007, 4438-4444.	2.0	14
119	The Role ofEscherichia coliform in the Biomineralization of Calcium Oxalate Crystals. European Journal of Inorganic Chemistry, 2007, 2007, 3201-3207.	2.0	13
120	The effect of the initial reactant molar ratio and doping with Fe3+ on the formation of calcium bilirubinate in water-oil microemulsions. Russian Journal of Physical Chemistry A, 2007, 81, 1141-1146.	0.6	0
121	Study on synthesis and properties of hydroxyapatite nanorods and its complex containing biopolymer. Journal of Materials Science, 2007, 42, 8599-8605.	3.7	21
122	Study on the preparation and formation mechanism of barium sulphate nanoparticles modified by different organic acids. Journal of Chemical Sciences, 2007, 119, 319-324.	1.5	48
123	Size- and Shape-Controlled Synthesis and Assembly of a Silver Nanocomplex in UV-Irradiated TSA Solution. European Journal of Inorganic Chemistry, 2006, 2006, 4658-4664.	2.0	12
124	Biomimetic Synthesis of Calcium Bilirubinate in Different Inverse Microemulsions. Synthesis and Reactivity in Inorganic, Metal Organic, and Nano Metal Chemistry, 2005, 35, 359-364.	0.6	7
125	Dynamic resource allocation and collaborative scheduling in R&D and manufacturing processes of high-end equipment with budget constraint. Optimization Letters, 0, , 1.	1.6	0